IOSR Journal of Applied Chemistry (IOSR-JAC)
e-ISSN: 2278-5736. Volume 7, Issue 4 Ver. II. (Apr. 2014), PP 50-56
www.iosrjournals.org

Computational Study on the Kinetics of Cl Initiated Oxidation of Methyl difluoroacetate ($CF_2HCOOCH_3$)

Laxmi Tiwari and Hari ji Singh
Department of Chemistry DDU Gorakhpur University Gorakhpur-273 009 (India)

Abstract: *The kinetics of hydrogen atom abstraction reactions of methyl difluoroacetate ($CF_2HCOOCH_3$) by Cl has been studied by quantum mechanical method. The structural optimization and frequency calculation of the titled compound was performed with density functional theory M062X with 6-311++G(d,p) basis set and energy values were calculated at G3 level of theory. IRC calculation was also performed to ascertain that the transition from reactant to product was smooth through the corresponding transition state. The rate constants were calculated using Canonical Transition State Theory (CTST) and the overall rate constant was found to be 8.09×10^{-13} cm^3 $molecule^{-1}$ s^{-1} for H atom abstractions of $CF_2HCOOCH_3$ by Cl. The calculated values are found to be in good agreement with the experimentally determined value of 2.03×10^{-13} cm^3 $molecule^{-1}$ s^{-1}.*
Keywords: *MDFA,G3 Method, M06-2X, IRC, Branching Ratios*

I. Introduction

Halogens have been determined to be responsible for depletion of stratospheric ozone resulting in the global warming. There are some halogen containing compounds such as chlorofluorocarbons (CFCs) is found to be responsible for the depletion of ozone layer in the stratospheric region of the atmosphere[1-4]. Therefore, attention has been directed to find suitable and environmental friendly replacements. A large number of compounds such as hydrochlorofluorocarbons (HCFCs), hydrofluorocarbons (HFCs), perfluorocarbons (PFCs) and hydrofluoroethers (HFEs) have been found to have similar physical properties as that of CFCs and these may suitably be used as an alternative in many industrial applications such as refrigerants, blowing and cleaning agents[5,6.] These possess almost zero ozone depletion potential due to absence of chlorine[7]. However, the presence of C-F bond in HFEs may enhance the strong absorption in the range 1000-3000 cm^{-1} that may cause a potential greenhouse effect[8,9]. HFEs have ether (─O─) linkage as a result of which they are highly reactive in the upper atmospheric region. It is found that the atmospheric oxidation of some HFEs leads to the formation of fluorinated esters as primary products[10-13] . The kinetics and mechanism of these fluoroesters formed from different types of HFEs in the atmosphere is not fully understood. A very little data is available in the literature regarding the destruction of these fluoroesters during its tropospheric oxidation by OH and Cl or other oxidizing species present in the atmosphere.

The kinetics of H-atom abstraction reaction of $CF_2HCOOCH_3$ by Cl radical has been studied by Blanco et al.[14] based on the relative rate method and products characterization by a gas chromatograph coupled with flame ionization detector. The rate constant at room temperature and atmospheric pressure has been determined to be $8.09\times10^{-13}cm^3$ $molecule^{-1}$ s^{-1}.

Detailed literature survey reveals that no theoretical studies has been performed on the titled molecule which is a primary ester formed during the HFE's degradation in the atmosphere. In the present work, we have performed theoretical calculations to understand the kinetics of degradation of $CF_2HCOOCH_3$ by Cl radicals. There are mainly two possible sites for the H-atom abstraction. These are shown as follows:

$$CF_2HCOOCH_3 + Cl \longrightarrow CF_2HCOOCH_2 + HCl \quad (R1)$$

$$CF_2HCOOCH_3 + Cl \longrightarrow CF_2COOCH_3 + HCl \quad (R2)$$

The thermochemical kinetics of the above two channels has been studied by DFT using a dispersion parameterized functional (M06-2X) developed by Truhlar's group[15,16] with 6-311++G(d,p) basis set. Canonical transition state theory (CTST) has been used to calculate the rate constant of the above two reaction channels [17]. Energy barrier used in determining the rate constant calculation was further refined by performing single point energy calculation using G3 level of theory[18].

II. Computatinal Method

All the electronic structure calculations of reactants, products and transition states for the reactions R1 and R2 were performed using GAUSSIAN 09 software package and the methods implemented therein[19]. Structures of reactant, products and transition states were optimized at DFT using a dispersion parameterized functional (M06-2X) developed by Truhlar's group[15,16] with 6-311++G(d,p) basis set.

The minimum energy path (MEP) for the reaction channels is checked by performing the intrinsic reaction coordinate (IRC) calculation at the same level of theory by making 15 point on both (reactant and product) sides of the transition state with the step size of 0.01 amu$^{1/2}$-bohr. The IRC plots for TS1 and TS2 are shown in Fig. 2. These plots show that the transition from the reactant to products was smooth through the respective transition state.

Vibrational frequencies were also calculated using the same level of theory at which structure optimization was made. All the stationary points had been identified to correspond to stable minima on the potential energy surface by ascertaining that all frequencies were real and positive. The transition states were characterized by the presence of only one imaginary frequency (NIMAG=1). To ascertain that the identified transition states connect reactant and products smoothly, intrinsic reaction coordinate (IRC) calculations[20] were performed at the same level. As the reaction energy barriers are very much sensitive to the level of the theory used during the calculation, the higher-order correlation corrected relative energies along with the density functional energies are necessary to obtain consistent reaction energies. Thus, single point energy calculation was performed at G3 level of theory[18].

Rate Constant

The rate constant calculation for reactions (R1) and (R2) was made using the canonical transition state theory (CTST)[21] which included a semi-classical one dimensional multiplicative tunneling correction factor using the following expression:

$$k = \Gamma(T)\frac{k_B T}{h}\frac{Q^{\ddagger}_{TS}}{Q_R}\exp\left(-\frac{\Delta E_0}{RT}\right) \quad (1)$$

where Γ(T) denotes tunnelling correction factor at temperature T, $Q^{\ddagger}_{TS}$and$Q_R$are the total partition function of transition state and reactants respectively. ΔE_0 is the barrier height determined as the energy difference between transition state and reactant. k_B, h and R are Boltzmann, Planck's, and the universal gas constants respectively. The tunnelling correction factor Γ(T) was calculated using computationally inexpensive Wigner's empirical method[22] given by the following expression:

$$\Gamma(T) = 1 + \frac{1}{24}\left(\frac{h\nu^{\#}}{k_B T}\right)^2 \quad (2)$$

where $\nu^{\#}$ is the imaginary frequency of the transition state and h and k_B have their usual meaning.

Partition function

The total partition functions of reactants and transition states to be used in the rate constant calculation using Eq. (1) were calculated at M062X/6-311++G(d,p) level of theory. The total partition function is approximated by the product of translational, rotational, vibrational, and electronic partition functions. Several low frequency vibrational modes were identified as internal rotations[23]. The total partition function of reactants [$CF_3C(O)OCH_2CF_3$] and transition states (TS1 and TS2) were corrected for hindered rotor as given by the following expression

$$Q_{corr} = \frac{Q_{HO}\cdot Q_{IR}}{\Pi Q_{v=i}} \quad (3)$$

where Q_{HO} is the harmonic oscillator partition function, Q_{IR} the internal rotation partition function and $Q_{v=i}$ is the partition function of normal mode vibrations corresponding to internal rotation.

The electronic partition functions of Cl atom were modified to take into account the splitting of their electronic level due to spin-orbit coupling. The ground $^2P_{3/2}$ (with degeneracy of 4) and excited $^2P_{1/2}$ (with degeneracy of 2) states of Cl atom are separated by an energy difference of 881 (cm^{-1}) [24]. Thus, Q_{elec} (Cl) is written as

$$Q_{elec}\,(Cl) = 4 + 2\exp(-881\ cm^{-1}.\ hc/kT) \quad (4)$$

III. Result and Discussion

Electronic structure. The optimized geometries of reactants ($CF_2HCOOCH_3$, Cl), products ($CF_2HCOOCH_2$, CF_2COOCH_3, HCl) and transition states (TS1 and TS2) for H-atom abstraction by Cl radical occurring through reactions R1 and R2 are determined at M062-X/6-311++G(d,p) level of theory and their harmonic vibrational frequency calculations were performed at the same level of theory. The optimized structures of the species involved during the H atom abstraction of the titled molecule by Cl are shown in Fig. 1. These structures also highlight a few important structural parameters. Results show that in the transition state TS1 corresponding to reaction channel R1, the breaking C-H bond stretched by about 28% (1.090Å to 1.391 Å) whereas the newly

forming HCl bond increased from 1.281Å to 1.465 Å (about 14%). Similarly, in the case of TS2 that corresponds to reaction channel R2, the breaking C-H bond stretched by about 20% (1.091 Å to 1.312Å) whereas the newly forming H-Cl bond increased from 1.281Å to 1.523Å (about 19%).

The results obtained during the frequency calculation are recorded in Table1. The imaginary frequency of transition states corresponding to the saddle point on the potential energy surface are found to be **944** cm^{-1}(TS1) and **1006** cm^{-1}(TS2). The larger absolute values of the imaginary frequency show that the transition states would be tight in nature. The spin contamination $<S^2>$ values of all the species involved in R1 and R2 are also listed in Table 1. The $<S^2>$ values for the doublets (radicals) vary from 0.752 to 0.759 before annihilation while $<S^2>$ value after annihilation for pure doublet is (0.75). This shows that the spin contamination for the title molecule does not have a significant role due to a slightly higher value than the expected.

The minimum energy path (MEP) for the reaction channels is checked by performing the intrinsic reaction coordinate (IRC) calculation at the same level of theory by making 15 point on both (reactant and product) sides of the transition state with the step size of 0.01 $amu^{1/2}$-bohr. The IRC plots for TS1 and TS2 are shown in Fig. 2. These plots show that the transition from the reactant to products was smooth through the respective transition state.

Energetics

Thermodynamic properties such as enthalpy of reaction (Δ_rH^0) and Gibbs free energy of reaction (Δ_rG^0) for both the reactions R1 and R2 are recorded in Table 3. Free energy values show that both reaction channels are exergonic in nature. The reaction enthalpy (ΔrH^0) values for reactions R1 and R2 are -2.56 and -5.99 kcal/mole , respectively, which clearly suggest that the product of reaction R2 is thermodynamically more favaurable than reaction R1. It reveal that both the reaction channels are thermodynamically facile. Thus, the hydrogen abstraction for reaction R2 may be thermodynamically more favorable than reaction R1 and the rate constant of reaction R2 will be expected faster than reaction R1. The barrier height for reaction R1 calculated at G3 is 2.32 kcal/mole .On the other hand the barrier height for reaction R2 calculated at G3 is 0.91 kcal/mole. These results show that the thermodynamic properties and the barrier heights calculated at G3 level give reliable result. Using the barrier heights evaluated at G3 level of calculations a potential energy diagram is constructed as shown in Fig. 4. This diagram shows the dominance of Cl initiated degradation process of $CF_2HCOOCH_3$ in the atmosphere.

Kinetics and Branching Ratio

The barrier heights (including zero-point energy) for reactions R1 and R2 are determined at G3 level of theory and an energy diagram is constructed as shown in Fig. 4. The results show that both of the reactions R1 and R2 proceed with positive barrier heights and therefore, both reaction channels are perceived to occur through direct mechanism (Reactant → TS → Products). The total partition functions involved in the rate constant calculation are corrected by hindered rotor partition function . Several low frequencies have been obtained during the harmonic vibrational frequency calculation as recorded in Table 1. Two low frequencies at 122 and 205 in the reactant, one low frequencies at 59 in TS1 and two low frequencies at 133 and 163 in TS2 have been identified as hindered rotors. The partition function corresponding to internal rotors are excluded from the harmonic oscillator partition function and hindered rotors are included to correct the total partition function for the reactant and the transition states using Eq. (3). The tunnelling correction factors Γ(T) for TS1 and TS2 have been calculated to be 1.97 and 1.79 respectively. A value of Γ(T) greater than 1 emphasizes that the H-atom may tunnel through the barrier with a greater probability than crossing the barrier height. The energy diagram shown in Fig. 4 reveals that the reaction channel R1 proceeds with a barrier height of 2.32 kcal/mol whereas the same for R2 is found to be 0.91 kcal/mol. This shows that reaction channel R2 is the dominant path for the H-atom abstraction by Cl for $CF_2HCOOCH_3$ molecule. The rate constants calculated from Eq. (1) is found to be 7.65 x 10^{-16} cm^3 $molecule^{-1}$ s^{-1} and 8.08 x 10^{-13} cm^3 $molecule^{-1}s^{-1}$ for R1 and R2 respectively. These results are also in accord with the potential energy diagram shown in Fig.4. The overall rate constant is determined using the following equation:

$$k_{overall} = k_{R1} + k_{R2} \qquad (6)$$

The overall rate constant thus determined is found to be 8.09 x 10^{-13} cm^3 $molecule^{-1}$ s^{-1} which is in close agreement with the experimental value of 2.48 x 10^{-13} cm^3 $molecule^{-1}$ s^{-1} obtained by Blanco et al. [11] using relative rate method and analyzing the reaction products by gas chromatograph coupled with flame ionization detector. The branching ratios (**Γ**) is computed as

$$\mathbf{\Gamma}_{path} = \frac{k_{path}}{k_{overall}} \times 100 \qquad (7)$$

The calculated value shows that reaction channel R2 contributes to about 99% to the overall reaction and thus it is concluded that the reaction channel R2 in which the H-atom is abstracted from the $–CF_2H$ group present in $CF_2HCOOCH_3$ is the dominant path during the atmospheric degradation of the titled ester during its reaction with Cl present abundantly in the troposphere

IV. Conclusion

We present here the potential energy profile (including geometries, energies and vibrational frequencies of reactant, transition states and products) and kinetic data for the $CF_2HCOOCH_3$ investigated at the G3//M06-2X/6-311G++(d,p) level of theory. The present investigation reveal that H-atom abstraction by Cl from the $–CF_2H$ group is the dominant path for its degradation in the atmosphere. The overall rate constant of 8.09×10^{-13} cm^3 $molecul^{-1}$ s^{-1} determined theoretically during the present investigation is found to be in close agreement with the experimental value of 2.03×10^{-13} cm^3 $molecul^{-1}$ s^{-1} obtained by Blanco et al.[14] using relative method. Further, the study also reveals that the meta density functional yield reliable thermochemical and kinetic data.

References

[1]. Solomon, S. Nature **1990**, 347 (6291), 347. doi:10.1038/347347a0.
[2]. Molina, M. J.; Rowland, F. S. *Nature* **1974,** 249 (5460)**,** 810.doi:10.1038/249810a0.
[3]. Rowland, F. S.; Molina, *M. J. Chem. Eng. News* **1994**, 8,72.
[4]. Weubbles, D. J. J. *Geophys. Res.* **1983,** 88 (C2), 1433.doi:10.1029/JC088iC02p01433.
[5]. Farman J. D, Gardiner B. G.; Shanklin J. D, *Nature* **1985** 315 ,207.
[6]. World Meterorological Organization (WMO). Scientific Assessment of Stratosphere Ozone: 1989; WMO, Global Ozone Research and Monitoring Project Report No.20,1991;WMO: Geneva, Switzerland; Vol.11.
[7]. Houghton, J. T. et al The Scientific Basis, Contribution of Working Group I to the Third Assessment Report of the Intergovernmental Panel on Climate Change, (IPCC), Geneva, **2001**.
[8]. Imasu R.; Suga. Matsuno A.; Meteorol T. J. Soc. *Jpn.* **73** 1123 (1995).
[9]. Blanco, M. B.; Bejan, I.; Barnes, I.; Wiesen, P.; Truel, M. *Environ. Sci. Technol*. **2010** 44, 2354
[10]. Oyaro, N.; Sellevag, S.R. Nielsen , C.J. *Environmental Science & Technology* **2004** 38, 5567
[11]. Ninomiya, Y.; Kawasaki, M.; Guschin, A.; Molina, L. T.; Molina, M. J.; Wallington, T. J. *Environmental Science & Technology*, **2000** 34, 2973.
[12]. Christensen, L. K.; Wallington, T. J.; Guschin, A.; Hurley, M. D.*J. Phys.Chem. A* **1999,**103, 4202.
[13]. Wallington, T. J.; Schneider, W. F.; Sehested, J.; Bilde, M.; Platz, J.; Nielsen, O. J.; Christensen, L. K.; Molina, M. J.; Molina, L. T.; Wooldridge, P. W. *J. Phys. Chem. A*, **1997**, 101, 8264.
[14]. Blanco, M.B.; Bejan, I.; Barnes, I.; Wiesen, P.; Truel, M. A. *Atmospheric Environment* **2008,** 18**,**453 .
[15]. Zhao, Y.; Truhlar, D. G. *J. Chem. Theory Comput.* **2008** 4, 1849.
[16]. Gonzalez, C.; Schlegel, H.B. *J. Chem. Phys*. **1990** 94, 5523.
[17]. Truhlar, D. G.; Garrett, B. C.; Klippenstein, S. J. *J. Phys. Chem*. **1996** 100 12771
[18]. Baboul, A.G.; Curtiss, L.A.; Redfern, P.C.; Raghavachari, K. *J. Chem. Phys*.**1999** 110, 7650.
[19]. M. J.; Frisch, et al. Gaussian 09 (Version C.01), Gaussian Inc, Wallingford, CT, **2010**
[20]. Frisch, M. J.; Trucks, G. W.; Schlegel, H. B.; Scuseria, G. E.; Robb, M. A.; Cheeseman, J. R., Scalmani, G.; Barone, V.; Mennucci, B.; Petersson , Nakatsuji, H.; Caricato, M.; X. Li, Hratchian, H. P.; Izmaylov, A. F; Bloino, J; Zheng, G.; Sonnenberg, J. L.; Hada, M.; Ehara, M.; Toyota, K.; Fukuda, R.; Hasegawa, J.; Ishida, M.; Nakajima, T.; Honda, Y.; Kitao, O.; Nakai, H.; Vreven, T.; Montgomery, J. A.; Peralta, Jr. J. E.; Ogliaro, F.; Bearpark, M.; Heyd, J. J.; Brothers, E.; Kudin, K. N.; Staroverov, V. N.; Keith, T.; Kobayashi, R.; Normand, J.; Raghavachari, K.; Rendell, A.; Burant, J. C.; Iyengar, S. S.; Tomasi, J.; Cossi, M.; Rega, N.; Millam, J. M.; Klene, M., Knox, J. E.; Cross, J. B.; Bakken, V.; Adamo, C.; Jaramillo, J.; Gomperts, R.; Stratmann, R. E.; Yazyev, O.; Austin, A. J.; Cammi, R.; Pomelli, C.; Ochterski, J. W.; Martin, R. L.; Morokuma, K.; Zakrzewski, V. G.; Voth, G. A.; Salvador, P.; Dannenberg, J. J.; Dapprich, S.; Daniels, A. D.; Farkas, O.; Foresman, J. B.; Ortiz, J. V.; Cioslowski, J., and Fox, D. J.; Gaussian 09 C.01 Gaussian, Inc.; Wallingford CT, **2010**.
[21]. Truhlar, D.G.; Garrett, B.C.; Klippenstein, S.J. *J. Phys. Chem*. **1996,** 100 (31), 12771 doi:10.1021/jp953748q.
[22]. Wigner, E.P. Z. *Phys. Chem*. **1932**, B19, 203.
[23]. Chuang, Y.Y.; Truhlar, D.G. *J. Chem. Phys*. **2000**,112**,** 1221
[24]. Chase, Davies,M. W. Jr.; Downey, C. A.; J. Frurip, R. Jr. McDonald, D. J. Syverud, R. A. A. N. Phys. Chem. Ref. Data, 14 1985

Table 1. Unscaled vibrational frequencies of reactants, products and transition states at the M062X/6-311++G(d,p) level of theory.

Species	Vibrational frequencies (cm^{-1})	$<S^2>$
$CF_2HCOOCH_3$	43, 122, 151, 205, 320, 346, 424, 582, 674, 830, 957, 1048, 1153, 1188, 1209, 1224, 1292, 1390, 1444, 1494, 1498, 1505, 1902, 3080, 3161, 3163, 3205	0.0
TS1	***944i,*** 35, 37, 59, 465, 203, 325, 350, 362, 435, 507, 579, 651, 809, 932, 942 , 978, 1119, 1172, 1212, 1220, 1237, 1265, 1395, 1438, 1468, 1936, 3127, 3149, 3257	0.754
TS2	***1006i,*** 45, 54, 110, 133, 163, 193, 253, 327, 372, 474, 608, 645, 845, 947, 1027, 1058, 1067, 1191, 1215, 1264, 1315, 1375, 1493, 1496, 1506, 1899, 3085, 3172, 3205	0.759
CF_2COOCH_3	108, 115, 160, 187, 196, 334, 402, 517, 644, 699, 869, 1048, 1190, 1210, 1250, 1402, 1476, 1499, 1508, 1545, 1802, 3082, 3163, 3196	0.755
$CF_2HCOOCH_2$	47, 151, 190, 211, 287, 339, 356, 436, 580, 654, 810, 942, 1121, 1163, 1202, 1217, 1288, 1391, 1432, 1464, 1912, 3150, 3212, 3373	0.754

HCl	3016	0.0
Cl	0	0.0

Table 2. Zero point corrected total energy of reactants, products and transition statesfor reaction R1 and R2(values are in Hartrees)

Species	**M062X**	**G3**
$CF_2HCOOCH_3$	-466.7541689	-466.6233289
$CF_2HCOOCH_2$	-466.0996822	-465.969186
CF_2COOCH_3	-466.1065649	-465.964760
TS1	-926.8856048	-926.6105943
TS2	-926.8861242	-926.6128378
HCl	-460.7898951	-460.654664
Cl	-460.1325607	-459.990959

Table 3 . Enthalpy of reaction (Δ_rH^0), Gibb's free energy of reaction (Δ_rG^0) and Gibb's free energy of activation ($\Delta_rG^{\#}$) for reaction channels R1 and R2 at 298 K (values are in kcal/mole)

Thermodynamic Parametre	**M062X/6-311++G(d,p)**		**G3**	
	R1	R2	R1	R2
Δ_rH^0	-1.31	-5.62	-2.56	-5.99
Δ_rG^0	-3.74	-7.88	-4.79	-8.00

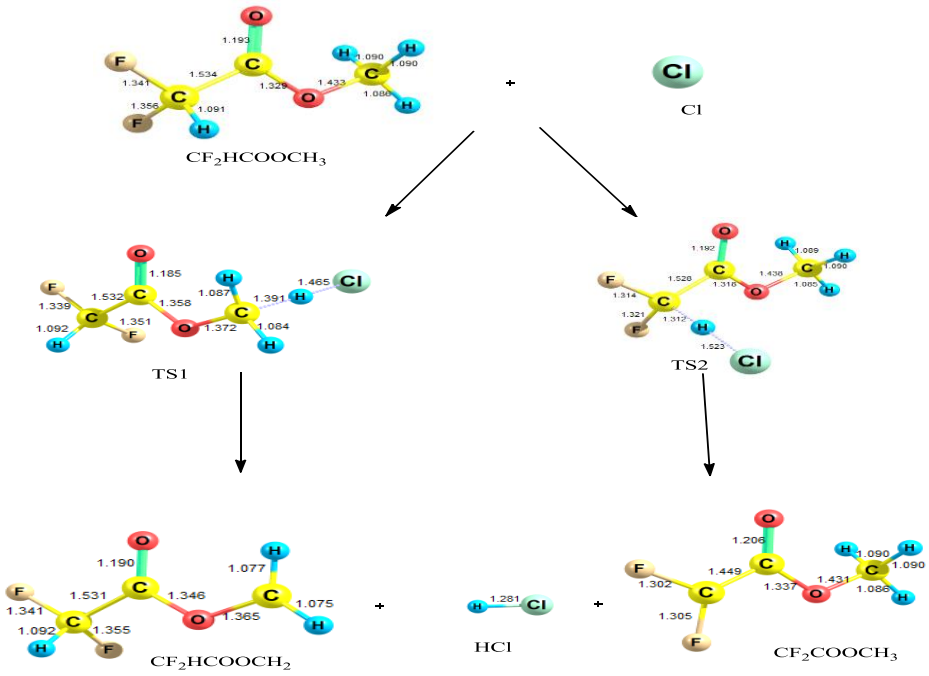

Figure1. Optimised geometries of reactants, products and transition states involved in the H atom abstraction reaction of $CF_2HCOOCH_3$ by Cl atom using M06-2X/6-311++G(d,p) level.

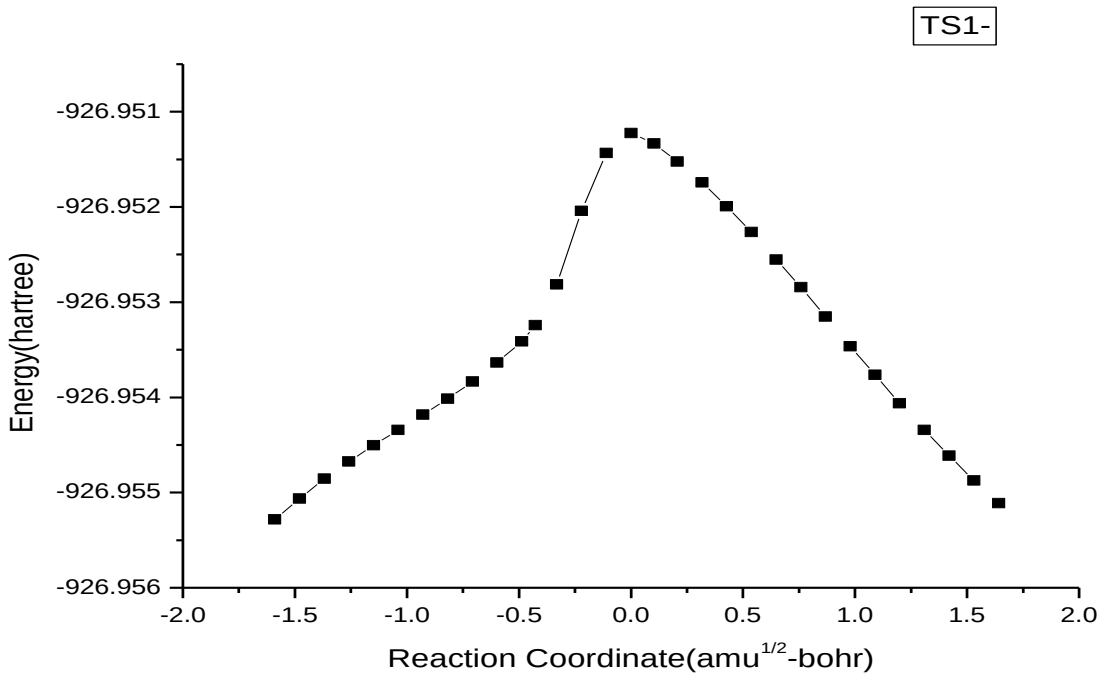

Figure 2. IRC plot for the transition state(TS1-Cl) involved in $CF_2HCOOCH_3$+Cl reaction at M062X/6-311++G(d,p) level of theory.

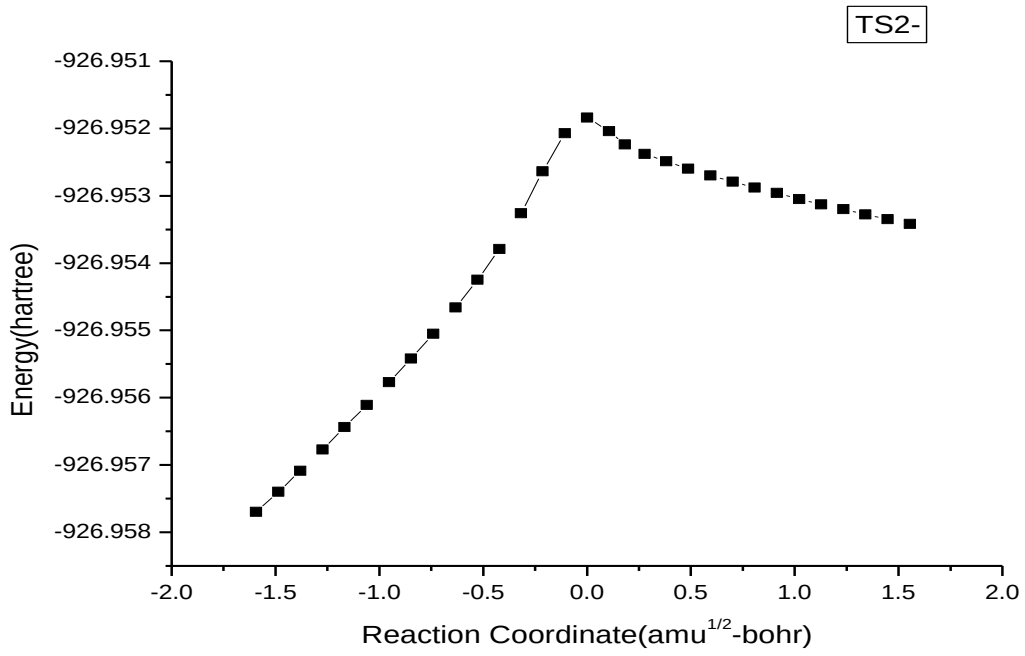

Figure 3. IRC plot for the transition state(TS2-Cl) involved in $CF_2HCOOCH_3$+Cl reaction at M062X/6-311++G(d,p) level of theory.

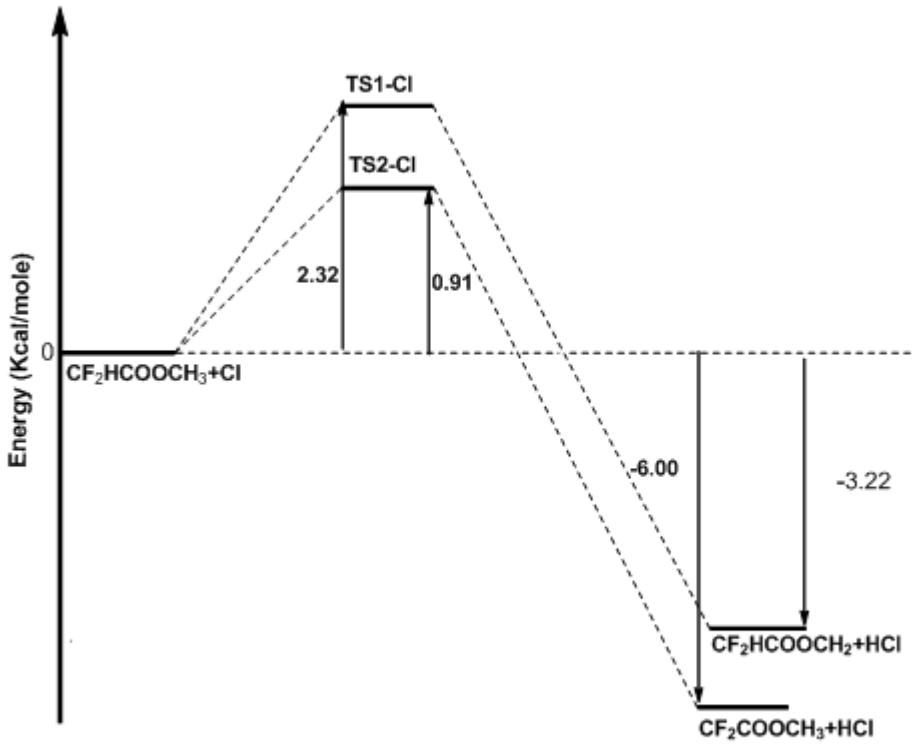

Figure 4. Schematic potential energy diagram for the reaction R1 and R2 at G3 level of theory